PRINCETON UNIVERSITY

DEPARTMENT OF AERONAUTICAL ENGINEERING

U. S. Army Transportation Research Command
Fort Eustis, Virginia

Project Number: 9R38-11-009-03
Contract Number: DA 44-177-TC-524

EFFECT OF C. G. POSITION, DUCT AREA RATIO AND DUCT ANGLE RATIO ON THE PERFORMANCE OF AN AERIAL JEEP, VTOL TYPE AIRARAFT

by

Joseph J. Traybar

Department of Aeronautical Engineering
Princeton University

Report No. 494 January 1960

Prepared by:

Joseph J. Traybar
Joseph J. Traybar
Research Assistant

Approved by:

Edward Seckel /J.T.
Edward Seckel
Associate Professor

CRD 360

FOREWORD

The research in this report was conducted by the Department of Aeronautical Engineering, Princeton University, under the sponsorship of the United States Army Transportation Research Command.

This work was performed by Messrs. P. Hampton and J. Traybar under the supervision of Professor E. Seckel, Department of Aeronautical Engineering, Princeton University, and was administered for the United States Army by Mr. H. Johnson of the Transportation Research Command.

TABLE OF CONTENTS

SUMMARY

Theoretical investigations are made on the performance of aerial jeep-type aircraft as influenced by various configuration changes. The primary objective of this report is the study of the relative effects on the power caused by selected design variations rather than the determination of the total power required for a specific vehicle. Attention is given to a configuration which utilizes ducted rotors in a triangular arrangement. It is assumed that the ducted rotors can be rotated with respect to the fuselage and that control is obtained by differential variations in thrust. The forward flight equilibrium equations are derived using simple momentum theory where duct angle of attack, exit slipstream velocity and forward speed are the variables. The specific quantities changed in order to determine their relative effects on the power are duct area ratio, duct angle of attack ratio and longitudinal center of gravity location.

I. INTRODUCTION

This research deals with a theoretical study of the performance of ducted propeller, aerial jeep-type aircraft as influenced by various design changes. The Army aerial jeeps (aerial platforms or sky-cars) are intended for use as VTOL, man carrying aircraft that will perform functions similar to ground jeeps. The envisioned requirements and general configurations of this class of vehicle are stated in detail in various papers (Refs. 1 through 5). In brief, some of the distinguishing features are: protection of rotating parts, silhouette of minimum dimensions, rotor system located below the level of the cockpit, 1000 pound payload and a cruise speed of about 50 knots as an acceptable minimum.

Several experimental vehicles of various designs have been developed. Generally, the different configurations incorporate ducted and unducted multi-rotor arrangements, utilizing vanes, cyclic pitch, collective and differential collective pitch for control. One design uses two ducted propellers in tandem while the other has an unducted rotor at each corner of a rectangular platform. Propulsion is obtained by tilting the entire machine nose-down so as to incline the thrust vectors forward.

Although the vehicles being developed have not been thoroughly flight tested to date, certain undesirable characteristics have been predicted from the data and material available. Some of the principal deficiencies noted on the ducted vehicles are strong nose-up pitching moments created in forward flight, large control required for trim, generally marginal stability and control and excessive vehicle attitude angles in forward flight. In addition, the desire for minimum vehicle size dictates the use of relatively high disc loadings with resultant high power requirements for small payloads.

The purpose of the research discussed in this report is to study the effect of selected configuration changes on the induced power rather than the determination of the total power required for specific vehicles. Attention is given to a ducted design typical of this class of vehicles but not necessarily patterned after existing machines. The machine studied in this report is a three duct triangular arrangement utilizing one duct forward and two ducts, laterally displaced, aft. An actual model designed along these lines and having rotating ducts is being fabricated by the NASA for wind tunnel testing at Langley Field.

The effects caused by flow interference among the ducted rotors are not included in this report because of the design selected. With the rear ducts separated laterally so that they are not directly immersed in the downwash of the front duct, it is assumed that large unfavorable flow interference would be minimized or perhaps eliminated by favorable flow or upwash.

Since interference effects are not included, this analysis is not restricted to the exact duct configuration selected. Only total front duct area and total rear duct area or the ratio of these areas and their respective longitudinal distance from the aircraft c.g. appear as terms in the equilibrium equations of this report.

A typical duct configuration is shown in Fig. 1. Ducted rotors of relatively high disc loadings are selected to minimize the over-all dimensions of the vehicle. It is assumed that these ducts can be rotated with respect to the fuselage. The ability to rotate the ducts with respect to the fuselage permits the fuselage to remain level in forward flight since the thrust vectors may be inclined forward without tilting the vehicles to extreme nose-down angles. The vehicle is controlled and trimmed by differential thrust.

Within the scope of this analysis, several selected configuration variations are made in order to determine their relative effects on the induced power. For a constant average disc loading, the parameters varied are the ratio of the front duct area to rear duct area, ratio of front to rear duct angle inclination with respect to fuselage and longitudinal center of gravity location. The effects caused by changing the average disc loading while holding the above mentioned parameters constant are also briefly analyzed.

These parameter variations were selected since it is not immediately obvious what the relative effects are on the induced power required in equilibrium forward flight for varying c.g. locations, duct areas and duct inclination angles.

In addition, a special case is considered for comparison of induced power required where the duct tilt angles and vehicle attitude are always equal to zero in forward flight. For this case, it is assumed that the ducted rotors provide lift and moment trim only, whereas propulsion is obtained by some auxiliary device or engine.

II. NOTATION

c_1 = #1 duct chord length (ft.) $c_1 = d_1$

c_2, c_3 = #2 and #3 duct chord length (ft.) $c_2 = d_2 = c_3 = d_3$

d_1 = #1 duct diameter (ft.) also basic dimension for l_t

d_2, d_3 = #2 and #3 duct diameter (ft.) $d_2 = d_3$

l_1 = longitudinal distance (ft.) between gross weight c.g. and line of action of front duct #1 lift force L_1

l_2 = longitudinal distance (ft.) between gross weight c.g. and line of action of rear duct lift forces L_2 and L_3

l_t = tail length (ft.) distance between front and rear duct centers and always equals $l_1 + l_2 = 3d_1 = l_t$

m_1 = mass flow through front duct (#1) $\rho S_1 V_{e_1}$ (slugs per sec.)

m_2, m_3 = mass flow through rear ducts #2 or #3 (slugs per sec.)

$m_2 = m_3$ or $\rho S_2 V_{e_2} + \rho S_3 V_{e_3} = 2m_2$

$C_L = \dfrac{L}{\rho S V_e^2}$ where, according to simple momentum theory,

$L = \rho S V_e (V_e \cos \alpha)$

and

$C_L = \cos \alpha$.

$C_D = \dfrac{D}{\rho S V_e^2}$ where, according to simple momentum theory,

$D = \rho S V_e (V_e \sin \alpha - V)$

and

$C_D = \sin \alpha - \dfrac{V}{V_e}$

NOTATION (continued

$C_M = \frac{M}{\rho S V_e^2 c}$ where, according to Ref. 6, the moment generated by a ducted propeller is

$M = \rho S V^2 c \cos \alpha \left(\frac{V_e}{V} - \sin \alpha\right)$

and

$C_M = \frac{V}{V_e} \cos \alpha - \left(\frac{V}{V_e}\right)^2 \cos \alpha \sin \alpha$

$C_W = \frac{W}{\rho S V_e^2}$ Weight coefficient

$D_m = mV - mV_e \sin \alpha$ Momentum drag (lbs.)

D_{m_i} = Momentum drag of individual ducts (lbs.)

F_p = Propulsive force (lbs.) measured along relative wind (V) direction

L_1 = Lift of front duct #1 (lbs.)

L_2, L_3 = Lift of rear ducts #2 and #3 (lbs.) $L_2 = L_3$

$2L_2$ = Lift of both rear ducts #2 and #3 (lbs.)

M_1 = Aerodynamic pitching moment of front duct #1 (ft.-lbs.)

M_2, M_3 = Aerodynamic pitching moment of rear ducts #2 and #3 (ft.-lbs.) $M_2 = M_3$

$2M_2$ = Aerodynamic pitching moment of both rear ducts #2 and #3 (ft.-lbs.)

$M_{c.g.}$ = Total pitching moment about c.g. (ft.-lbs.)

P = Power (ft.-lbs. per sec. or horsepower)

R = Duct radius (ft.)

S_1 = Exit area of front duct #1 ($ft.^2$)

S_2,S_3 = Exit area of rear ducts #2 and #3 ($ft.^2$) $S_2 = S_3$

S_F = Total front duct exit area ($ft.^2$) $S_F = S_1$

NOTATION (continued)

S_R = Total rear duct exit area (ft.^{2}) $S_R = S_2 + S_3 = 2S_2$

S = Total area of all ducts (ft.^{2}) $S = S_1 + S_2 = S_3 = S_F + S_R$

T_i = Thrust force measured along duct axis

T_i/S_i = Disc loading or thrust loading where i = 1, 2, or 3

V = Flight velocity (ft. per sec.)

V_{e_i} = Duct exit slipstream velocity (ft. per sec.) where i = 1, 2, or 3 and $V_{e_2} = V_{e_3}$

W = Gross weight of machine (lbs.) (3000)

$\frac{W}{S}$ = Average disc loading where S is total disc area (lbs. per ft.^{2})

α = Duct angle of attack (In this study it is equal to the angle between the duct and fuselage reference lines) (degrees)

θ = Vehicle attitude angle (angle measured between fuselage reference line and horizon and in this report equals zero for the case where the ducts rotate and fuselage remains level to horizon) (degrees)

ρ = Air mass density (slugs per cubic ft.)

III. ANALYSIS

The objective of this research is the study of the effects of selected configuration changes on the induced power required for forward flight.

1. Assumptions:

For the limited scope of this study it is possible to make certain important assumptions and considerations in order to simplify the analysis. The powerful effects caused by flow interference among the ducted rotors are not included because of the design selected. By separating the rear ducts laterally so that they are not directly immersed in the downwash of the front duct, it is presumed that any large unfavorable effects would be minimized or even eliminated by favorable flow or upwash.

Considerations involving duct efficiency or internal and parasite drag are not included since the objective of this study is the determination of the relative effects on power as selected parameters are varied and not the calculation of the total power required for a specific vehicle.

It is assumed that the fuselage remains level in forward flight since all ducts can be rotated with respect to the fuselage. Also, for the relatively slow speeds considered, the crew, cockpit, supporting structure and fuselage contribute no additional forces and moments.

Use is made of simple momentum theory which as applied to ducted fans includes the assumptions that the duct prevents slipstream contraction and the cross-sectional area and velocity of the slipstream at infinity are equal to the cross-sectional area and velocity of the slipstream at the duct exit.

The expression for the pitching moment generated by a ducted propeller in non-axial forward flight is utilized as derived in Ref. 6.

2. Vehicle notation and parameter variations.

Fig. 1 represents the typical arrangement for the aerial jeep of this report. The top view shows one duct (#1) at the front of the machine with duct diameter equal to d_1, and the other two ducts (#2 and #3), laterally displaced, at the rear with diameter d_2 always equal to d_3. The basic dimension l_t between the centers of the front and rear ducts is always $3d_1$, where d_1 is the diameter of the front duct. The side view shows l_1 and l_2 as the distances between the respective lift vectors and the location of the gross weight c.g. of the machine. The standard position of the c.g. is arbitrarily located so that the machine is in moment equilibrium in hovering for the condition where the disc loadings of the individual ducts are all equal. The forward flight velocity of the machine is equal to V and the duct chord lengths are equal to c. Duct angle of attack α is the angle measured between the fuselage and duct reference lines and can be varied by rotating the ducts as desired providing that the individual thrusts are adjusted so that equilibrium conditions are maintained. The duct exit slipstream velocities are represented by V_e and are directed along the duct axis. Duct thrust is measured along the duct axis and is represented by

$$T = mV_e = \rho S V_e^2 \qquad (1)$$

where

$$m = \rho S V_e. \qquad (2)$$

The lift vectors L, act perpendicular to the flight velocity V and are equal to

$$L = T \cos \alpha \tag{3}$$

The pitching moment or couple generated by the ducted propeller in forward flight is represented by M where (Ref. 6)

$$M = \rho S V^2 c \cos\alpha \left(\frac{V_e}{V} - \sin\alpha\right) \tag{4}$$

The total moment about the c.g. is

$$M_{c.g.} = M_1 + M_2 + M_3 + l_1 L_1 - l_2 L_2 - l_2 L_3 = 0 \tag{5}$$

or

$$M_{c.g.} = M_1 + 2M_2 + l_1 L_1 - 2l_2 L_2 = 0 \tag{6}$$

For the investigations considered, a gross weight of 3000 pounds and an average disc loading of 50 pounds per square foot are assumed. These quantities fix the total disc area of the vehicle at 60 square feet.

One of the parameters varied in this analysis is the duct area ratio (S_T/S_R or S_1/S_2) or the distribution of the total disc area between the front and rear rotors. (Table I)

TABLE I

Case	Area Ratio S_1/S_2 or S_F/S_R		Front Area ft.^{2} S_1	Rear Area ft.^{2} S_2	S_3	d_1	$d_{2,3}$	l_1	l_2
I	0.75	0.375	16.4	21.8	21.8	4.56	5.27	9.96	3.73
II	1.0	0.5	20	20	20	5.05	5.05	10.09	5.05
III	2.0	1.0	30	15	15	6.18	4.37	9.27	9.27
IV	3.0	1.5	36	12	12	6.77	3.91	8.12	12.18
V	4.0	2.0	40	10	10	7.13	3.57	7.13	14.27
VI	6.0	3.0	45	7.5	7.5	7.57	3.09	5.67	17.03

where

$$\frac{W}{S} = 50 \text{ lbs./ft.}^2 \qquad W = 3000 \text{ lbs.}$$

$$S_F = S_1 \qquad S_R = S_2 + S_3 \qquad (7)$$

$$S = S_1 + S_2 + S_3 = 60 \text{ ft.}^2$$

$$l_t = l_1 + l_2 = 3d_1$$

As area ratios change, the length l_t of the vehicle always equals $3d_1$. This means that the tail length l_t changes as the front duct diameter changes for the various area ratios since $l_t = l_1 + l_2 = 3d_1$. For each area ratio the standard center of gravity location is such that the disc loadings of all ducts are equal in hover.

A second parameter variation is c.g. movement with respect to the standard location for a given area ratio. The individual disc loadings will no longer be equal in hover. The effect of varying c.g. position on the power was studied by moving the c.g. in one foot increments (changing the distances l_1 and l_2) both fore and aft of the standard location. In this report, the center of gravity position for a given case does not vary with forward speed.

The remaining parameter variation is the duct angle ratio $\frac{\alpha_2}{\alpha_1}$ or $\frac{\alpha_R}{\alpha_F}$. Since the front and rear duct angles can be controlled, they may be programmed at any arbitrary but fixed rate as $\frac{\alpha_2}{\alpha_1} = K$. When K is equal to one, the front duct angle is always equal to the rear duct angle. In addition to investigating the effects on power at other values of K, studies were made for the case where the duct angles are programmed in a manner that the momentum drag of each individual ducted rotor is equal to zero. The condition of individual momentum drag equilibrium for each ducted rotor is discussed in the next section.

3. Force diagram for a single duct.

Fig. 2a shows a vector diagram of forces for a single duct inclined at an angle alpha with respect to the vertical and having a forward velocity V and an exit slipstream velocity V_e. The incoming momentum is represented by $m\bar{V}$ drawn from the point of action P on the actuator disc. The ducted rotor deflects the flow through an angle and energy is added by the actuator disc so that the exit momentum is $m\bar{V}_e$ directed along the duct axis. The change in momentum is represented by $m\bar{V}_e - m\bar{V}$ and produces the resultant force in the opposite direction labeled R.F.

In level equilibrium flight, the total pitching moment must be zero and the vertical component of the resultant force R.F. represents the lift force which must equal the weight. Since no parasite drag is being considered, the drag condition for equilibrium is satisfied when the net momentum drag on the system is equal to zero. In this report, the momentum drag D_m is defined as the force produced in the horizontal direction (in line with the relative wind) due to turning the air through an angle through the ducted rotor and is equal to the horizontal component of the resultant force R.F. or

$$D_m = mV - mV_e \sin \alpha \qquad (8)$$

In Fig. 2a, the indicated duct inclination and exit momentum produce a resultant force that has a horizontal component F_H (forward propulsion or negative drag) so that the net momentum drag is not equal to zero and therefore the individual ducted system shown is not in momentum drag equilibrium. However, if the exit momentum and duct angle are of proper value so that the resultant force is vertical (Fig. 2b),

i.e. the horizontal component of the resultant force equals zero ($D_m = 0$), the ducted rotor is said to be in momentum drag equilibrium. (If parasite drag were being considered, Fig. 2a could be thought of as an equilibrium diagram for a single ducted propeller for the case where the horizontal component of the resultant force would exactly counteract the parasite drag force, so that the net drag on the system would equal zero.)

For vehicles utilizing a combination of the ducted rotors inclined at arbitrary angles, it is possible for the momentum drag of each ducted rotor to be positive, zero, or negative and the vehicle still remain in drag equilibrium. This may be accomplished in one of two ways.

In the first case, the individual ducts are able to rotate differentially as required to keep the momentum drag of each duct equal to zero. In forward flight, the ducted rotors produce a net nose-up pitching moment about the c.g. that must be trimmed to zero by differential thrust for equilibrium. In order to counteract the nose-up moment, the exit velocity of the front duct (V_{e_1}) is decreased and that of the rear duct (V_{e_2}) is increased (Fig. 1). If the condition $D_{m_i} = 0$ (Fig. 2b) is to be maintained, the tilt angle (α_1) of V_{e_1} must increase and the tilt angle (α_2) of V_{e_2} must decrease so that the resultant force (R.F.) of each duct is vertical and therefore remains in momentum drag equilibrium.

In the second case, the ducts are not individually in momentum drag equilibrium but are coupled together and rotate at various fixed rates as $\alpha_2 = K\alpha_1$. The momentum drags of the ducts are both positive and negative and the drag equilibrium condition for the vehicle is satisfied when the sums of all the momentum drags collectively total zero.

In this report, frequent use is made of the notation $D_{m_i} = 0$ which means that the momentum drag of each individual ducted rotor is always equal to zero. Use of $\alpha_2 = K\alpha_1$ or $D_{m_i} \neq 0$ means that the ducts are collectively in drag equilibrium and the sum of the momentum drags acting on the machine equal zero. To satisfy the drag equilibrium conditions, the net momentum drag of the vehicle must always equal zero. Solutions to the equilibrium equations were obtained for both cases.

Also, from the vector diagram the expressions for lift and drag according to simple momentum theory are

$$L = \rho S V_e (V_e \cos \alpha) \tag{9}$$

$$D = \rho S V_e (V_e \sin \alpha - V) \tag{10}$$

If C_L and C_D are defined as

$$C_L = \frac{L}{\rho S V_e^2} \tag{11}$$

$$C_D = \frac{D}{\rho S V_e^2} \tag{12}$$

then C_L and C_D become

$$C_L = \cos \alpha \tag{13}$$

$$C_D = \sin \alpha - \frac{V}{V_e} \tag{14}$$

Using the expression for the pitching moment generated by a ducted propeller as derived in Ref. 6

$$M = \rho S V^2 c \cos \alpha \left(\frac{V_e}{V} - \sin \alpha\right) \tag{4}$$

and defining

$$C_M = \frac{M}{\rho S V_e^2 c} \tag{16}$$

the pitching moment coefficient for this case becomes

$$C_M = \frac{V}{V_e}\cos\alpha - \left(\frac{V}{V_e}\right)^2 \cos\alpha \sin\alpha \tag{17}$$

The coefficients C_L, C_D, and C_M so defined are utilized in the derivation of the equilibrium equations.

4. Equilibrium equations

In level, forward flight, equilibrium, the total lift created by all ducts must equal the gross weight of the machine and the propulsive force must equal the drag (net drag equals zero). Also the pitching moment created by the ducted rotors in forward flight must be trimmed so that the net moment about the c.g. equals zero.

The three simultaneous equilibrium equations for lift, drag and pitching moment are expressed in terms of exit velocities, duct angles, physical dimensions, weight and forward velocity. The quantities c_1, c_2, d_1, d_2, l_1, l_2, S_1, S_2 and W are always known and the remaining quantities are the variables V_{e_1}, V_{e_2}, α_1, α_2, and V.

The equilibrium equations may be written as

Lift Equation

Referring to Fig. 1, the equilibrium lift equation, where the total lift must equal the gross weight of the machine, is

$$L_1 + L_2 + L_3 = W \tag{18}$$

or

$$L_1 + 2L_2 = W \tag{19}$$

Using equations 1, 2 and 3, the lift equation (19) becomes

$$\rho S_1 V_{e_1}^2 \cos \alpha_1 + 2 \rho S_2 V_{e_2}^2 \cos \alpha_2 = W \tag{20}$$

Since (Equation 13)

$$C_{L_1} = \cos \alpha_1 \quad \text{and} \quad C_{L_2} = \cos \alpha_2 \tag{21}$$

Equation (20) becomes

$$W = C_{L_1} \rho S_1 V_{e_1}^2 + 2 C_{L_2} \rho S_2 V_{e_2}^2 \tag{22}$$

Non-dimensionalizing by $\rho S_2 V_{e_2}^2$ the lift equation in final form is

$$C_W = C_{L_1} \frac{S_1}{S_2} \left(\frac{V_{e_1}}{V_{e_2}} \right)^2 + 2 C_{L_2} \tag{23}$$

Drag equation

The equilibrium drag equation, where the total momentum drag acting on the vehicle is equal to zero, is

$$D_1 + D_2 + D_3 = 0 \tag{24}$$

or

$$D_1 + 2D_2 = 0 \tag{25}$$

where $D = mV - mV_e \sin \alpha$ (Equation 8).

Therefore, Equation (25) becomes

$$m_1 V - m_1 V_{e_1} \sin \alpha_1 + 2 \left[m_2 V - m_2 V_{e_2} \sin \alpha_2 \right] = 0 \tag{26}$$

and using former notation

$$\rho S_1 V_{e_1}^2 \left(\sin \alpha_1 - \frac{V}{V_{e_1}} \right) + 2 \rho S_2 V_{e_2}^2 \left(\sin \alpha_2 - \frac{V}{V_{e_2}} \right) = 0 \tag{27}$$

Since (Equation 14).

$$C_{D_1} = \sin \alpha_1 - \frac{V}{V_{e_1}} \quad \text{and} \quad C_{D_2} = \sin \alpha_2 - \frac{V}{V_{e_2}} \tag{28}$$

then Equation (27) becomes

$$C_{D_1} \rho S_1 V_{e_1}^2 + 2C_{D_2} \rho S_2 V_{e_2}^2 = 0 \tag{29}$$

Non-dimensionalizing by $\rho S_2 V_{e_2}^2$, the drag equation is

$$C_{D_1} \frac{S_1}{S_2} \left(\frac{V_{e_1}}{V_{e_2}} \right)^2 + 2 C_{D_2} = 0 \tag{30}$$

Moment equation

The pitching moment equation is

$$M_{c.g.} = M_1 + 2M_2 + l_1 L_1 - 2l_2 L_2 = 0 \tag{6}$$

where M denotes the aerodynamic pitching moment for a single ducted rotor in forward flight. For the moment equation, use is made of an expression for the pitching moment of a single duct as derived in Ref. 6 where

$$M = \rho S V^2 c \cos \alpha \left(\frac{V_e}{V} - \sin \alpha \right) \tag{4}$$

Using equations 1, 3 and 4, the pitching moment equation becomes (sub. in Equation 6)

$$\rho S_1 V^2 c_1 \cos \alpha_1 \left(\frac{V_{e_1}}{V} - \sin \alpha_1 \right) + 2 \rho S_2 V^2 c_2 \cos \alpha_2 \left(\frac{V_{e_2}}{V} - \sin \alpha_2 \right) + l_1 \rho S_1 V_{e_1}^2 \cos \alpha_1 - 2 l_2 \rho S_2 V_{e_2}^2 \cos \alpha_2 = 0 \tag{31}$$

Since (by Equations (13) and (17))

$$C_{L_1} = \cos \alpha_1 \qquad C_{L_2} = \cos \alpha_2 \tag{13}$$

$$C_{M_1} = \frac{V}{V_{e_1}} \cos \alpha_1 - \left(\frac{V}{V_{e_1}} \right)^2 \cos \alpha_1 \sin \alpha_1 \qquad C_{M_2} = \frac{V}{V_{e_2}} \cos \alpha_2 - \left(\frac{V}{V_{e_2}} \right)^2 \cos \alpha_2 \sin \alpha_2 \tag{17}$$

and rearranging and non-dimensionalizing by $\rho S_2 V_{e_2}^2 c_2$ the moment equation takes the form

$$C_{M_1} \frac{S_1}{S_2} \left(\frac{V_{e_1}}{V_{e_2}} \right)^2 \left(\frac{c_1}{c_2} \right) + 2C_{M_2} + C_{L_1} \frac{S_1}{S_2} \left(\frac{V_{e_1}}{V_{e_2}} \right)^2 \frac{l_1}{c_1} \frac{c_1}{c_2} - 2C_{L_2} \frac{l_2}{c_2} = 0 \tag{32}$$

The equilibrium equations listed together are

FORWARD FLIGHT

Lift Equation

$$W = \rho S_1 V_{e_1}^2 \cos \alpha_1 + 2 \rho S_2 V_{e_2}^2 \cos \alpha_2 \tag{20}$$

Drag Equation

$$0 = \rho S_1 V_{e_1}^2 \left(\sin \alpha_1 - \frac{V}{V_{e_1}} \right) + 2 \rho S_2 V_{e_2}^2 \left(\sin \alpha_2 - \frac{V}{V_{e_2}} \right). \tag{27}$$

Moment Equation

$$\begin{aligned} 0 = {} & \rho S_1 V^2 c_1 \cos \alpha_1 \left(V_{e_1}/V - \sin \alpha_1 \right) \\ & + 2 \rho S_2 V^2 c_2 \cos \alpha_2 \left(V_{e_2}/V - \sin \alpha_2 \right) \\ & + l_1 \rho S_1 V_{e_1}^2 \cos \alpha_1 - 2 l_2 \rho S_2 V_{e_2}^2 \cos \alpha_2 \end{aligned} \tag{31}$$

or in non-dimensional form

FORWARD FLIGHT

Lift Equation

$$C_W = C_{L_1} \frac{S_1}{S_2} \left(\frac{V_{e_1}}{V_{e_2}} \right)^2 + 2 C_{L_2} \tag{23}$$

Drag Equation

$$0 = C_{D_1} \frac{S_1}{S_2} \left(\frac{V_{e_1}}{V_{e_2}} \right)^2 + 2 C_{D_2} \tag{30}$$

Moment Equation

$$0 = C_{M_1} \frac{S_1}{S_2} \left(\frac{V_{e_1}}{V_{e_2}} \right)^2 \frac{c_1}{c_2} + 2 C_{M_2} + C_{L_1} \frac{S_1}{S_2} \left(\frac{V_{e_1}}{V_{e_2}} \right)^2 \frac{l_1}{c_1} \cdot \frac{c_1}{c_2} - 2 C_{L_2} \frac{l_2}{c_2} \tag{32}$$

HOVERING

Lift Equation

$$C_W = \frac{S_1}{S_2} \left(\frac{V_{e_1}}{V_{e_2}} \right)^2 + 2 \tag{33}$$

Moment Equation

$$0 = \frac{S_1}{S_2} \left(\frac{V_{e_1}}{V_{e_2}} \right)^2 l_1 - 2 l_2 \tag{34}$$

The level, forward flight, equilibrium equations of the subject aerial jeep are three non-linear simultaneous equations in the five flight or trim variables V_{e_1}, V_{e_2}, α_1, α_2 and V (Equations (20), (27) and (31)). The quantities W, ρ, S_1, S_2, c_1, c_2, l_1 and l_2 are known for each selected case.

For the specific scope of this report, a fourth equation is obtained for the case where the ducts are geared together and rotate at various fixed rates as $\alpha_2 = K \alpha_1$. Selecting K for the particular case to be studied, one angle may be chosen as a parameter and specifies the flight condition. Therefore, the value of the other angle is automatically known. The three original equations ((20), (27) and (31)) will have only three variables (V_{e_1}, V_{e_2} and V) for which unique solutions may be obtained since all other quantities are known.

For comparison, another case was studied where the ducts are always in individual momentum drag equilibrium ($D_{m_i} = 0$). While it is admitted that a design where the ducts maintain individual momentum drag equilibrium seems impractical, the case is analyzed since it provides an optimum condition with which to compare other results. Therefore, the drag equation (Equation 27) may be written as two separate equations for $D_{m_1} = 0$.

$$D_{m_1} = m_1 V - m_1 V_{e_1} \sin \alpha_1 = 0 \tag{35}$$

$$D_{m_2} = m_2 V - m_2 V_{e_2} \sin \alpha_2 = 0 \tag{36}$$

or

$$\sin \alpha_1 - \frac{V}{V_{e_1}} = 0 \tag{37}$$

$$\sin \alpha_2 - \frac{V}{V_{e_2}} = 0 \tag{38}$$

Now there are four equations ((20), (37), (38) and (31)) with the five flight or trim variables V_{e_1}, V_{e_2}, α_1 , α_2 and V. Unique solutions may be obtained by selecting a value for one variable and thereby specifying the flight condition or forward speed.

Actual closed form analytic solutions of the equations were not attempted since it appeared simpler to obtain solutions, consistent with the accuracy required for this analysis, by iterative methods. The iterative procedures used to solve the equations are fully outlined in the Appendices.

5. Power equation

The power equation may be expressed as the change in slipstream kinetic energy (Δ KE) where

$$P = \Delta \text{ KE} =$$

$$= (1/2)\, m_1(V_{e_1}^2 - V^2) + (1/2)\, m_2(V_{e_2}^2 - V^2) + (1/2)\, m_3(V_{e_3}^2 - V^2) \quad (39)$$

or

$$P = (1/2)\, m_1(V_{e_1}^2 - V^2) + m_2(V_{e_2}^2 - V^2) \quad (40)$$

Using previous notation and rearranging, the power equation takes the form

$$P = (1/2)\rho S_1 V_{e_1}^3 \left(1 - \frac{V^2}{V_{e_1}^2}\right) + \rho S_2 V_{e_2}^3 \left(1 - \frac{V^2}{V_{e_2}^2}\right) \quad (41)$$

where all the quantities are specified or determined by solutions to the simultaneous trim equations.

6. Special Case

A special case (Fig. 9) is considered for comparison of power required where the duct tilt angles and vehicle attitude are always equal to zero in forward flight ($\alpha = \Theta = 0$). This means that the fuselage always remains level but the ducts do not tilt or rotate and provide lift and moment trim only. In this case, propulsion is assumed to be obtained by some auxiliary device or engine that provides a forward thrust force in the horizontal direction through the center of gravity.

The equilibrium lift and moment equations for forward flight in this specia case are

SPECIAL CASE FORWARD FLIGHT ($\alpha = \Theta = 0$)

Lift

$$W = \rho S_1 V_{e_1}^2 + 2 \rho S_2 V_{e_2}^2 \tag{42}$$

Moment

$$0 = \rho S_1 c_1 V V_{e_1} + 2 \rho S_2 c_2 V V_{e_2} + l_1 \rho S_1 V_{e_1}^2 - 2 l_2 \rho S_2 V_{e_2}^2 \tag{43}$$

The drag equation takes a slightly different form since this auxiliary propulsive force F_P must equal the total momentum drag of the vehicle at each forward speed in order to satisfy the equilibrium condition.

The drag equation is

$$F_P = \rho S_1 V V_{e_1} + 2 \rho S_2 V V_{e_2} \tag{44}$$

The lift and moment equations are solved graphically for the unknowns V_{e_1} and V_{e_2} for each desired forward speed V. Knowing V_{e_1} and V_{e_2}, F_P may be obtained for each forward speed selected (Eq. (44)).

The total power required for forward flight is the sum of the power required for lift, moment trim and propulsion and is given by

$$P_{total} = P_{lift\ \&\ moment} + P_{propulsion} \tag{45}$$

where

$$P_{lift\ \&\ moment} =$$

$$= 1/2\ \rho\ S_1 V_{e_1}^{3} \left[1 - \frac{V^2}{V_{e_1}^2}\right] + \rho\ S_2 V_{e_2}^{3} \left[1 - \frac{V^2}{V_{e_2}^2}\right] \tag{46}$$

$$P_{propulsion} = FP \cdot V \tag{47}$$

IV. DISCUSSION

For the limited scope of this report, certain assumptions are made in order to simplify the analysis of the effects on power caused by changes in the configuration of the vehicle. These assumptions are outlined and explained in the ANALYSIS.

In addition to these assumptions, certain important conditions and considerations were imposed on the problem. The gross weight of the machine (3000 pounds) and the average disc loading ($\frac{W}{S}$ = 50 lbs./ft.^{2}) are fixed. Therefore, the total disc area of the vehicle is constant and always equal to 60 sq. ft. For the different area ratios, the standard center of gravity location is always exactly positioned so that all ducts have equal disc loadings in hover. When c.g. position is selected as the quantity to be varied, the c.g. location is moved fore and aft with respect to this standard location and therefore, the ducts will no longer have equal disc loadings in hover. Center of gravity position does not vary with forward speed. The length of the vehicle or tail length l_t is always equal to $3d_1$, where d_1 is the diameter of the front duct for the particular area ratio being studied. The duct angles are programmed at various fixed rates $\alpha_2 = K\alpha_1$ except for

the case when the ducts are always in individual momentum drag equilibrium ($D_{m_i} = 0$). Equilibrium conditions are maintained by thrust variations.

Because of the numerous variables involved and the selection of various other quantities that are allowed to change value in a prescribed way, it is important to remember these conditions, notations and assumptions when interpreting the results shown in the graphs.

1. AREA RATIO VARYING

In Fig. 3a, power is plotted versus forward speed for several of the selected area ratios (black curves, S_F/S_R = 0.375, 0.5, 1.5 and 3.0). The average disc loading is equal to 50 and the ducts are in individual momentum drag equilibrium ($D_{m_i} = 0$). As a result of the method of locating the c.g. for each area ratio (equal disc loadings at hover), the power at hover is the same for all area ratios. The different area ratios plotted all show a reduction in power as forward speed increases (increased mass flow effect). The largest reduction in power occurs for an area ratio S_F/S_R equal to 1.5 and, for example, at V equal to 60 feet per second the power is approximately 3% less than the value at hover. Note that values of S_F/S_R greater or less than 1.5 do not provide as great a reduction in power.

In Fig. 3a, the red curves represent a cross-plot of the black curves at two selected velocities (V equals 30 and 60 feet per second). For these curves the velocity is held constant and power is plotted versus area ratio. From each of these red curves it is possible to determine the optimum area ratio for minimum power at a selected speed.

At both selected velocities the optimum value of S_F/S_R is approximately equal to 1.5 (circled points) or S_F = 36 ft.^{2}, S_R = 24 ft.^{2}, where S_1 = 36, S_2 = 12, and S_3 = 12 (Table I).

Because of the various assumptions and conditions imposed on this problem, the exact reasons for the existence of an optimum area ratio for minimum power may not be immediately evident and the following discussion is offered.

If the pitching moment created by the ducted rotors were zero for all area ratios, at any given forward speed the individual thrusts or exit velocities would always be equal. Therefore, the power required would be a constant value because there would be no changes required in the front or rear duct thrusts or exit velocities for pitching moment trim purposes. Inspection of the power equation (Eq. (41)) reveals that power will increase as exit velocities become more dissimilar in order to trim existing pitching moments.

Now suppose that, at a given forward speed, the pitching moment created by the ducted rotors were a constant value and did not vary with changes in duct area or area ratio. In that case, it would be possible to determine whether the power required to trim a constant pitching moment had a minimum value for a certain area ratio by investigating the power as S_F/S_R approached extreme values (where $S_F/S_R \rightarrow 0$ and ∞).

If S_F/S_R approached infinity, the area of the front duct S_F would approach 60 square feet and the area of the rear ducts would approach zero square feet. Since the tail length always equals $3d_1$, l_t would be some finite length (approximately 26 feet). With the zero area rear ducted rotor, infinite power would be needed to produce a finite force at the finite tail length in order to provide the required trim pitching moment.

If, on the other hand, the area ratio approached zero, the area of the front duct would approach zero square feet and the area of the rear ducts would approach 60 square feet. Since the diameter of the front duct would be zero, the tail length would be zero ($l_t = 3d_1$). The front and rear ducts would now be superimposed on one another. For this case, doubly infinite power would be needed to produce the required pitching moment for trim because of the zero tail length and infinite disc loading.

If the length of the vehicle were a finite quantity (l_t equal to $3d_1$ or even a constant value), the power required to trim a given pitching moment caused by a specified total duct area would be infinite at both extremes of area ratio so that a minimum does exist at some intermediate value of S_F/S_R.

According to this discussion, whenever the total disc area and vehicle length are specified, there exists an optimum area ratio that gives a minimum power condition at a given speed when the pitching moment is a constant value and does not vary with area ratio.

However, the expression utilized for the pitching moment created by a single ducted rotor (Eq. (4)) shows that, for a given speed, the pitching moment does vary as a function of the individual duct area S. As duct areas change, the pitching moment will vary and exit velocities (and consequently the power) must be adjusted in order to maintain equilibrium.

Therefore, the previously determined optimum area ratio corresponding to the minimum power condition (where the pitching moment was assumed a constant value and not a function of S_F/S_R) will be influenced by the variation in pitching moment with area ratio.

The red curves of Fig. 3a show the variation of power at a given speed as area ratio changes.

2. DUCT ANGLE RATIO VARYING

In Fig. 3b, power is plotted versus forward speed for several selected duct angle ratios (black curves, $\frac{\alpha_2}{\alpha_1} = K$, where K = 0.5, 0.7, 1.0 and 1.5). The average disc loading $\frac{W}{S}$ is still equal to 50 pounds per square foot and the area ratio $S_F/S_R = 1.5$ is selected as the optimum from Fig. 3a and is held constant. Since the ducts are programmed at some arbitrary but fixed rate, the ducts are not individually in momentum drag equilibrium, however, collectively the momentum drag of the system is equal to zero. This means that the duct exit velocity vectors are so inclined that one duct may have positive momentum drag and the others negative, but the total drag equals zero to satisfy the drag equilibrium condition.

For comparison the curve representing $D_{m_i} = 0$ and $S_F/S_R = 1.5$ (Fig. 3a) is plotted on Fig. 3b. From Fig. 8a it can be determined that for $D_{m_i} = 0$ the value of the duct angle ratio K is approximately between 0.8 and 0.9.

The curves again show a reduction in horsepower with increasing forward speed (mass flow effect) that varies with duct angle ratio. The curve representing equal duct angles $\alpha_2 = \alpha_1$, K = 1 has the same plot as K = 0.7 and very closely approximates the results obtained for the curve $D_{m_i} = 0$. At 60 feet per second the power represented by these curves is approximately 3% less than the value at hover.

The red curves (Fig. 3b) are again a cross plot of the black curves at two selected velocities (V equal to 30 and 60 ft. per second). The optimum value of K is on the order of 0.85 (circled points) which approximates the value for the condition $D_{m_i} = 0$.

3. CENTER OF GRAVITY LOCATION VARYING

In Fig. 3c, power is plotted versus forward speed for several different center of gravity locations (black curves for c.g. movement fore and aft of standard position). The average disc loading $\frac{W}{S}$ is still equal to 50 pounds per square foot, $D_{m_i} = 0$, and the optimum area ratio of S_F/S_R equal to 1.5 (Fig. 3a) is still utilized. The black curve labeled "STANDARD" is identical to the curve in Fig. 3a where the center of gravity is so located that all ducts have equal disc loading in hovering. The other black curves represent center of gravity movement from this standard location so that the disc loadings of the ducts are no longer equal in hovering. Center of gravity locations remain fixed along each curve as labeled, i.e., center of gravity locations do not vary with forward speed.

Note that the power increases in hovering as the center of gravity is moved fore or aft of the standard location where disc loadings are equal. Movement of the c.g. causes changes in individual disc loadings and differential exit velocities, thereby causing an increase in power.

For forward flight, it is beneficial to refer to the cross plots (red curves) in order to interpret the effect of c.g. movement. In hover, the minimum power is obtained for the c.g. located in the standard position where disc loadings are all equal. At 30 feet per second the optimum c.g. position is approximately one foot forward of the standard location (circled point). At 60 feet per second the optimum is approximately 2 feet forward.

C. G. travel is not ordinarily acceptable as a control. However, the center of gravity may be located to give optimum disc loadings for minimum power at hover or any forward speed as desired.

4. AVERAGE DISC LOADING VARYING

Fig. 4 shows the effect of changing average disc loading on α, V_e, V_{e_1}/V_{e_2}, and power versus forward speed. These effects have been shown previously in other studies or texts for single duct designs. Briefly stated, Fig. 4 shows that power, exit velocity and exit velocity ratio V_{e_1}/V_{e_2} all increase while duct angle of attack decreases as the disc loading is increased.

Special note should be taken of the trends associated with average disc loading (Fig. 4d). It is obvious that power increases with higher disc loadings but of more interest to this study is the trend of the reduction in power with slow forward speeds for different disc loadings. At the lower disc loadings the induced power drops off quite rapidly even at low forward speeds. At the higher disc loadings, this reduction is less noticeable and, in fact, becomes insignificant for low forward speeds up to 50 miles per hour. In this respect, it seems difficult to obtain any significant reductions in induced power for relatively slow forward speeds whenever high disc loadings are utilized.

5. POWER DISTRIBUTION TO FRONT AND REAR DUCTS

Fig. 5 shows the division of the total induced power plotted in Fig. 3 for the three varying cases. In this graph the solid and broken lines show how the total power is distributed between the front and rear duct systems. The sum of these two curves gives the total power as plotted in Fig. 3. In all cases shown, the power for the front duct decreases and for the rear ducts increases with forward speed.

6. VALUES OF EXIT VELOCITY AND EXIT VELOCITY RATIO

Figs. 6 and 7 show the values of exit velocity ratio V_{e_1}/V_{e_2} and exit velocity V_e versus forward speed for the varying cases. In Figs. 6c and 7c, the symbols (circles) show the points where the exit velocities are approximately equal and consistent with the minimum point conditions of c.g. movement shown in Fig. 3c where $V_{e_1} \approx V_{e_2}$ at 30 feet per second for c.g. one foot forward and $V_{e_1} \approx V_{e_2}$ at 60 feet per second for c.g. two feet forward.

7. VALUES OF DUCT ANGLE OF ATTACK

Fig. 8 similarly shows the values of the duct angles. Only the front duct angle is plotted in Fig. 8b since the rear angle can be obtained by the relationship $\alpha_2 = K \alpha_1$. In Fig. 8c, for purposes of clarity, the scales for the front and rear duct angles are separated so that superimposed curves are avoided.

8. SPECIAL CASE ($\alpha = \theta = 0$)

In Fig. 9 the results are plotted for the special case mentioned in the ANALYSIS. Power is plotted versus forward speed and the average disc loading is equal to 50 pounds per square foot and the area ratio is equal to 1.5.

Curve A is the optimum plot from Fig. 3a where $S_F/S_R = 1.5$ and $D_{m_i} = 0$. For the equilibrium curve A, the fuselage remains level and the duct angles and exit velocities are of such value that each duct is in individual momentum drag equilibrium. The c.g. for all curves are located so that the ducts have equal disc loadings in hover.

Curve B is obtained from the solution of Equation (46), where the values of V_{e_1} and V_{e_2} are obtained by solving the lift and moment

Equations (42) and (43). This curve represents the power required for lift and moment trim only, when the fuselage remains level and the ducts are not tilted ($\theta = \alpha = 0$). The power required for forward propulsion is not included in this curve.

The propulsive force required for forward speed is obtained by solving Equation (44) using the values of V_{e_1} and V_{e_2} obtained from the solution of Equations (42) and (43). The power required for propulsion is obtained by Equation (47) and is represented in Fig. 9 by the difference between curve B and C, where C is Equation (45) and represents the total induced power required for forward flight when $\theta = \alpha = 0$. Note that at 60 feet per second the power increase of curve C over curve A is relatively large (on the order of 25% increase).

V. CONCLUSIONS

Attempts to gain significant reductions in the induced power of aerial jeep-type aircraft are difficult since it is known that, for the given speed range, the reduction of induced power with increasing forward speed becomes smaller as average disc loadings become larger.

For the subject ducted rotor vehicle in the optimum configuration of the varied parameters, there is only a small reduction in induced power with forward speed. The induced power required for forward flight is primarily influenced by the disc loading. If the effect of parasite power is added, the small beneficial effect obtained by the reduction in induced power is minimized. The total power would be essentially constant or increased for the forward speeds considered.

From the analysis, the optimum area ratio of front duct area to rear duct area was determined to be approximately 1.5, i.e., the front duct area is 1.5 times as large as the rear duct area for minimum power at the forward speeds considered.

Programming the rotating ducts so that they have equal angles with respect to the fuselage very closely approximates the optimum duct angle configuration for minimum power.

When longitudinal center of gravity is varied, the optimum position is obtained whenever the center of gravity is located so that the thrust loadings of all ducts are equal. Consequently, the center of gravity may be positioned to give a minimum power condition at hover or any one forward speed as desired.

REFERENCES

1. Hewin, Larry M., "What is Required of the Aerial Jeep?" Presented at the SAE Annual Meeting, January 12-16, 1959 Report 10R.

2. McKinney, M. O. "Stability and Control of the Aerial Jeep." Presented at the SAE Annual Meeting, January 12-16, 1959 Report 10S

3. Evans, Robert W., "Aerophysics Aerial Platform." Presented at the SAE Annual Meeting, January 12-16, 1959 Report 10T

4. Gorton, John V., "The Chrysler Aerial Jeep Project." Presented at the SAE Annual Meeting, January 12-16, 1959 Report 10U

5. Piasecki, F. N., "The Development of the Piasecki 'Sky-Car'." Presented at the SAE Annual Meeting, January 12-16, 1959 Report 10V

6. Sacks, Alvin H. "The Flying Platform as a Research Vehicle for Ducted Propellers." Presented at the 26th annual meeting, Institute of the Aeronautical Sciences, January 27-30, 1958

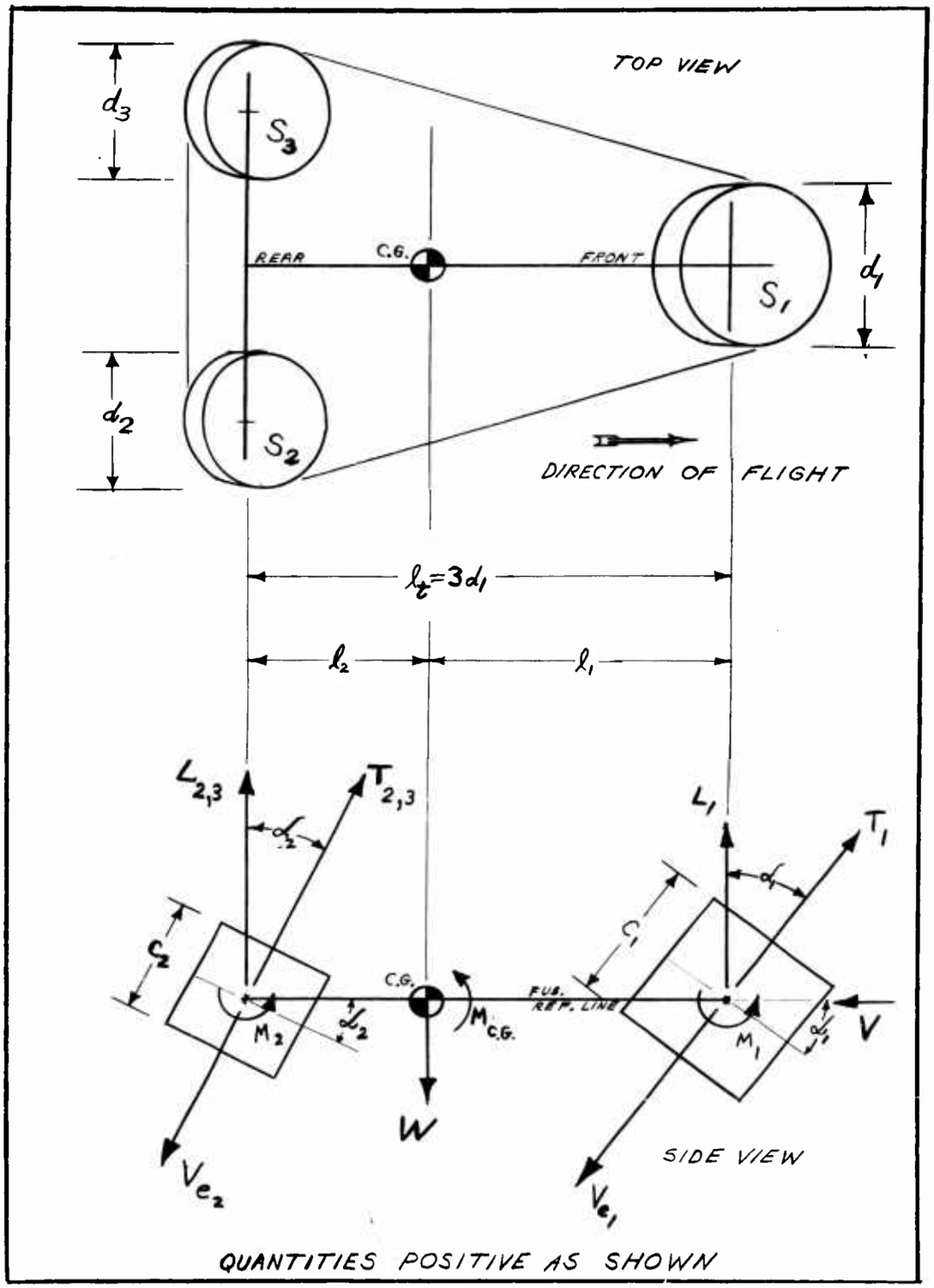

FIG. 1 VEHICLE NOTATION

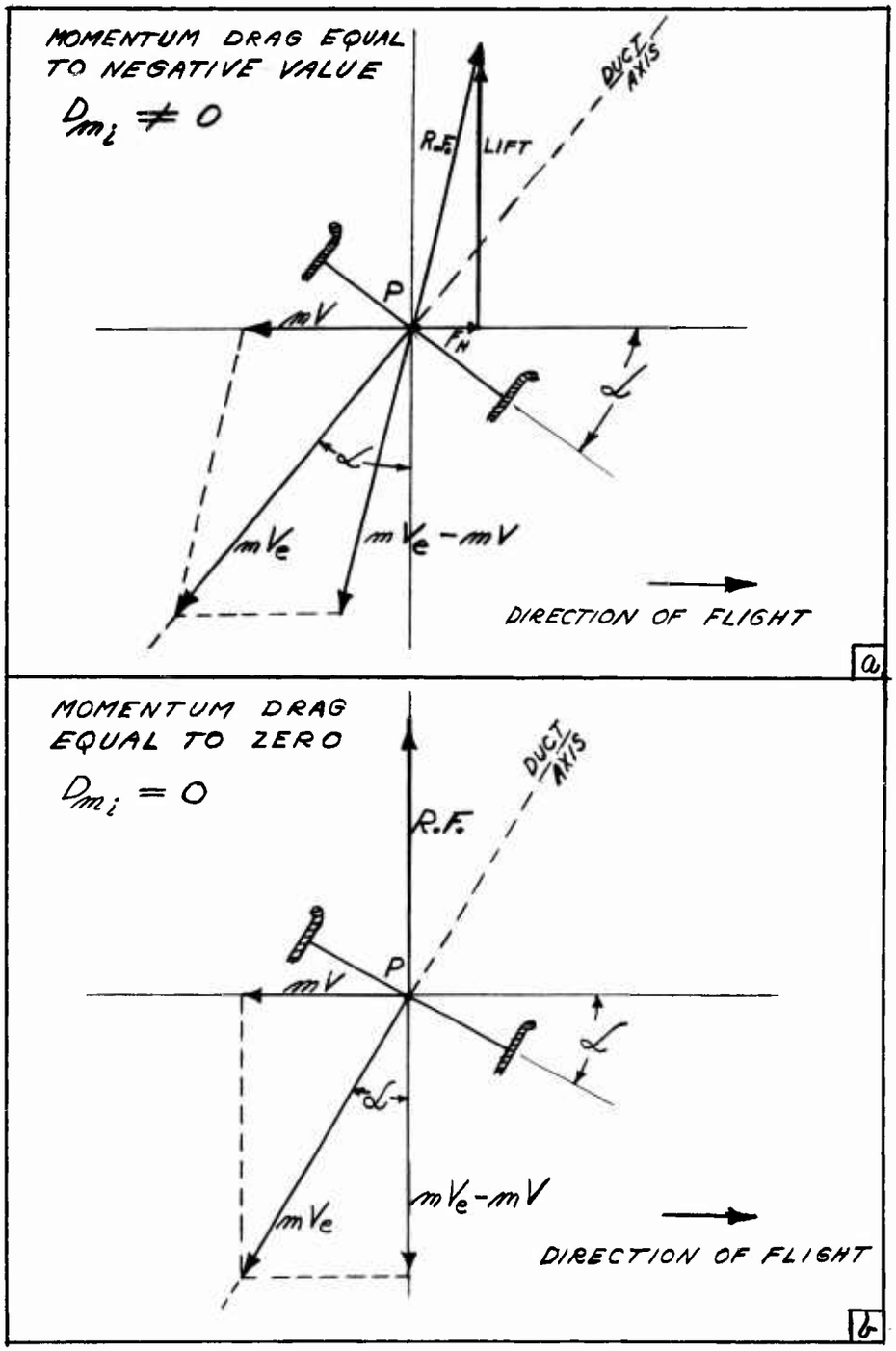

FIG. 2 VECTOR DIAGRAM FOR SINGLE DUCT

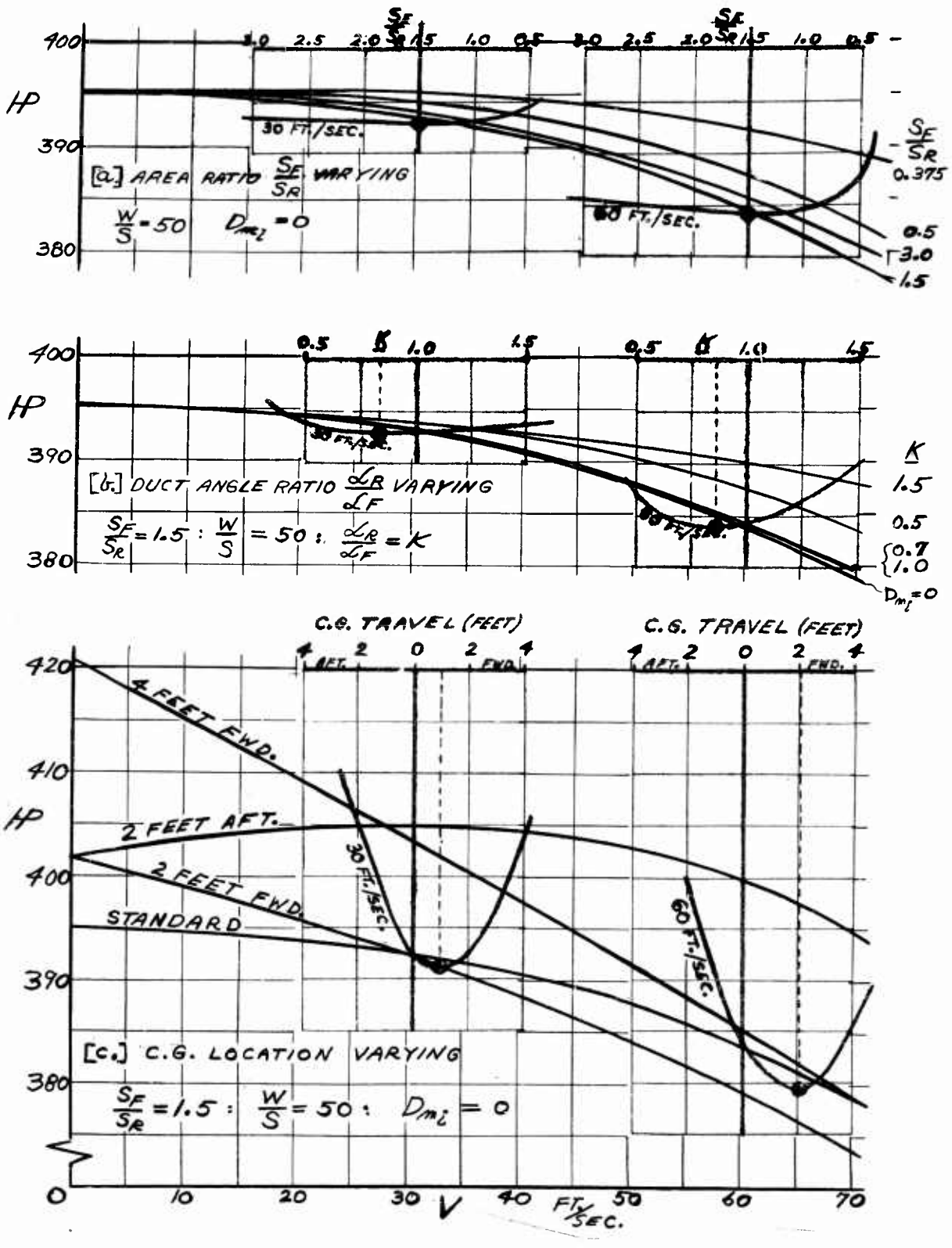

FIG. 3 INDUCED POWER vs. FORWARD VELOCITY

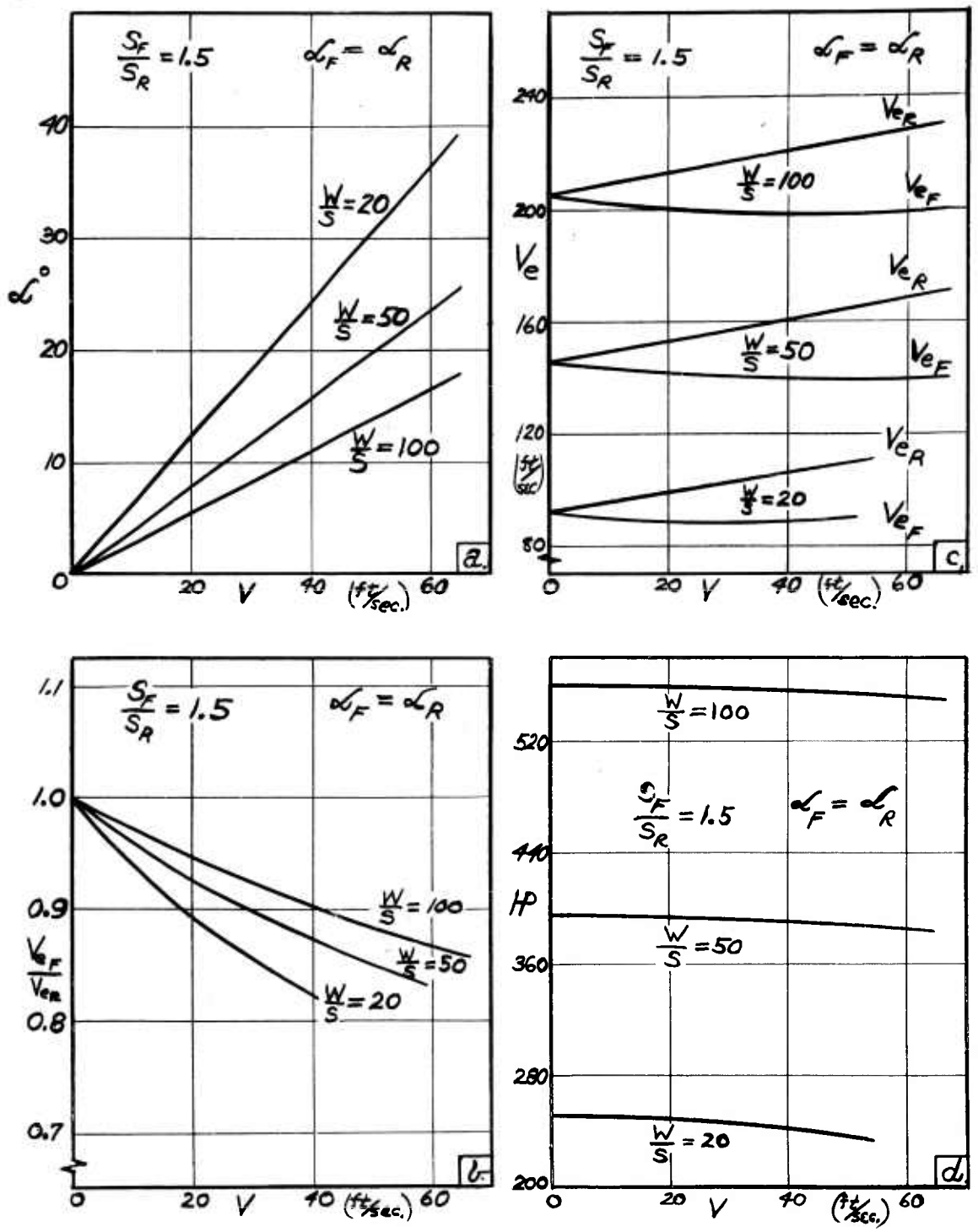

FIG. 4 EFFECT OF DISC LOADING ON PERFORMANCE AND TRIM VS. FORWARD VELOCITY

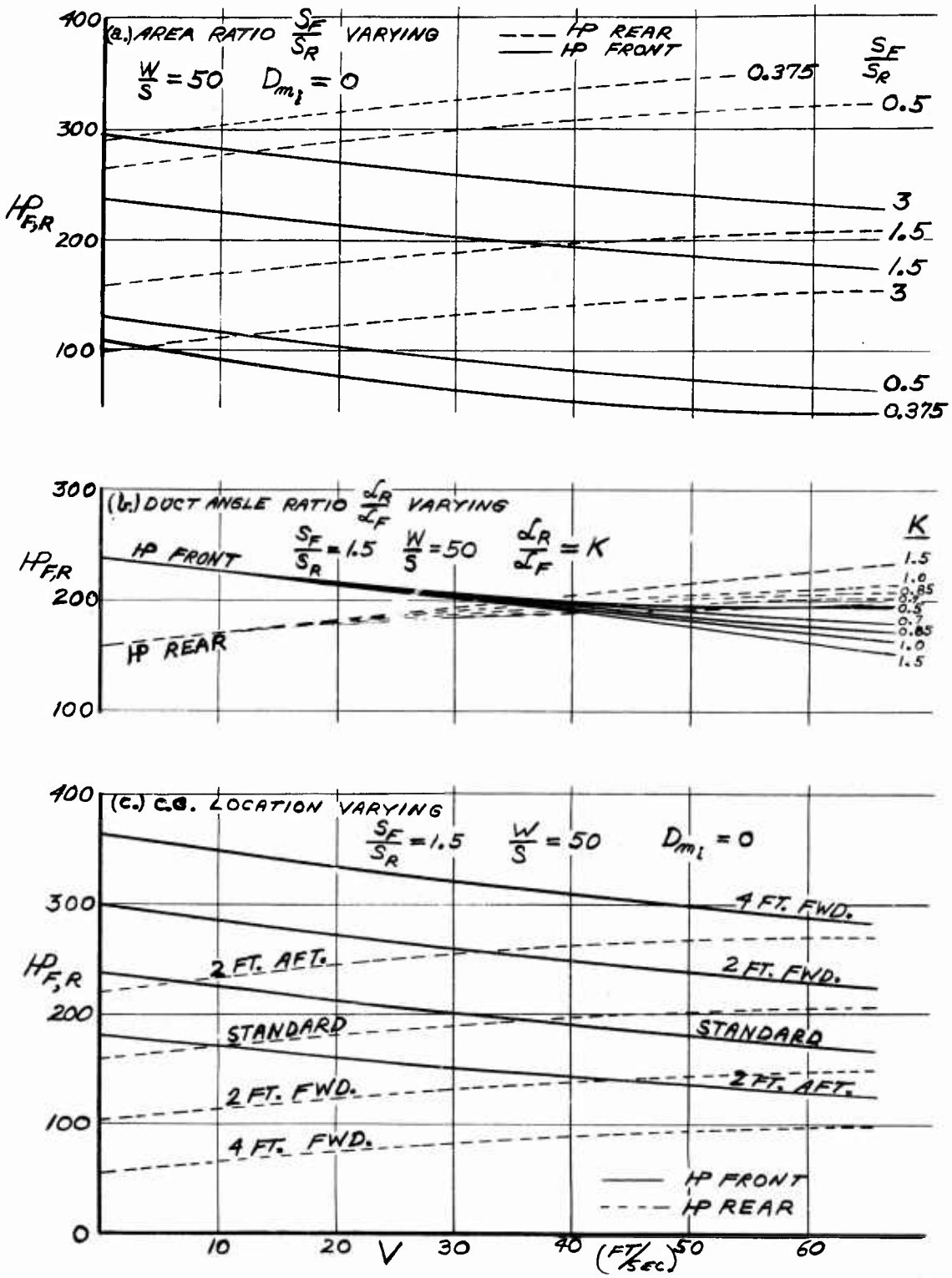

FIG. 5 INDUCED POWER TO FRONT OR REAR DUCTS VS. FORWARD VELOCITY

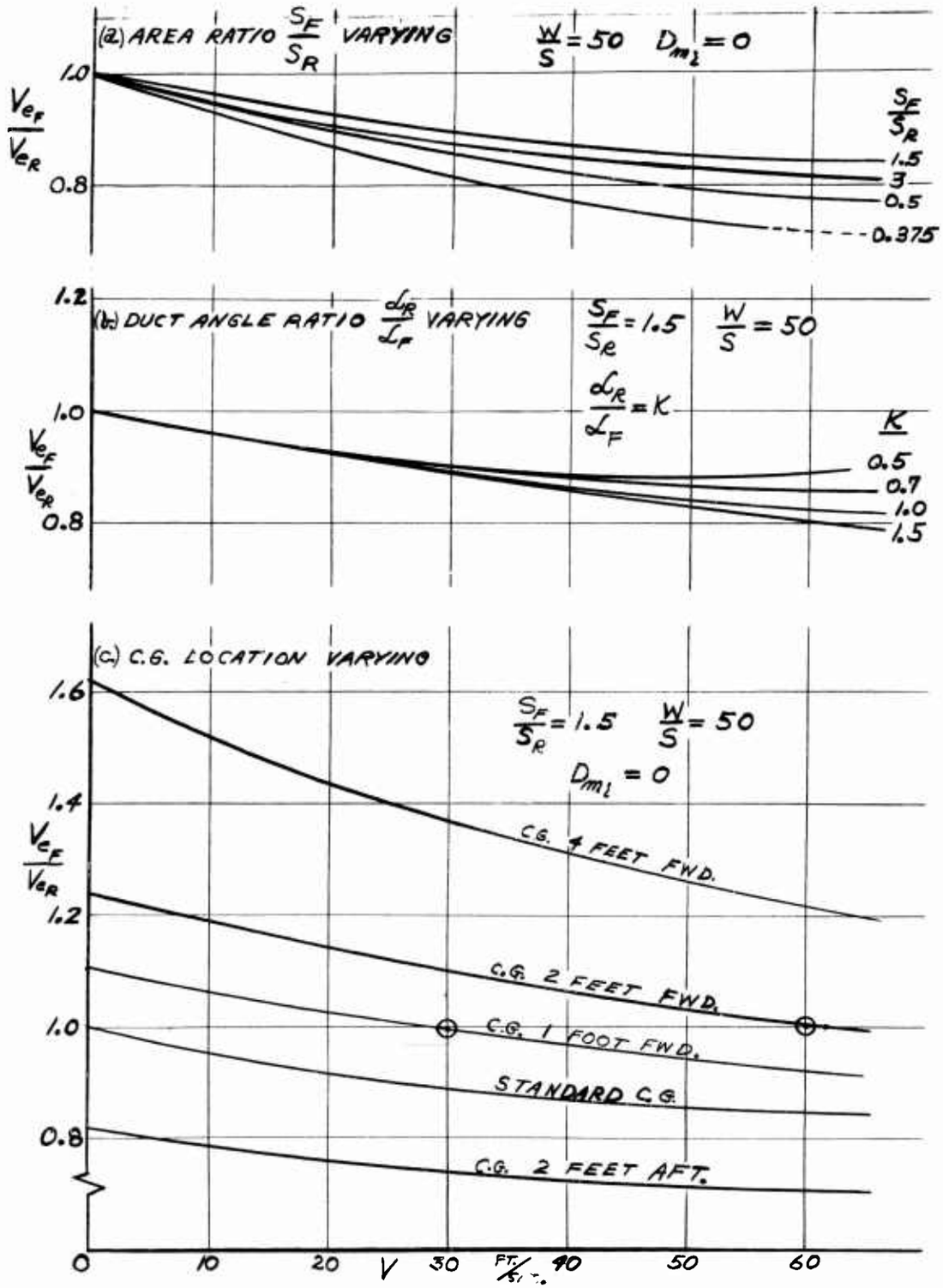

FIG. 6 EXIT VELOCITY RATIO VS. FORWARD SPEED

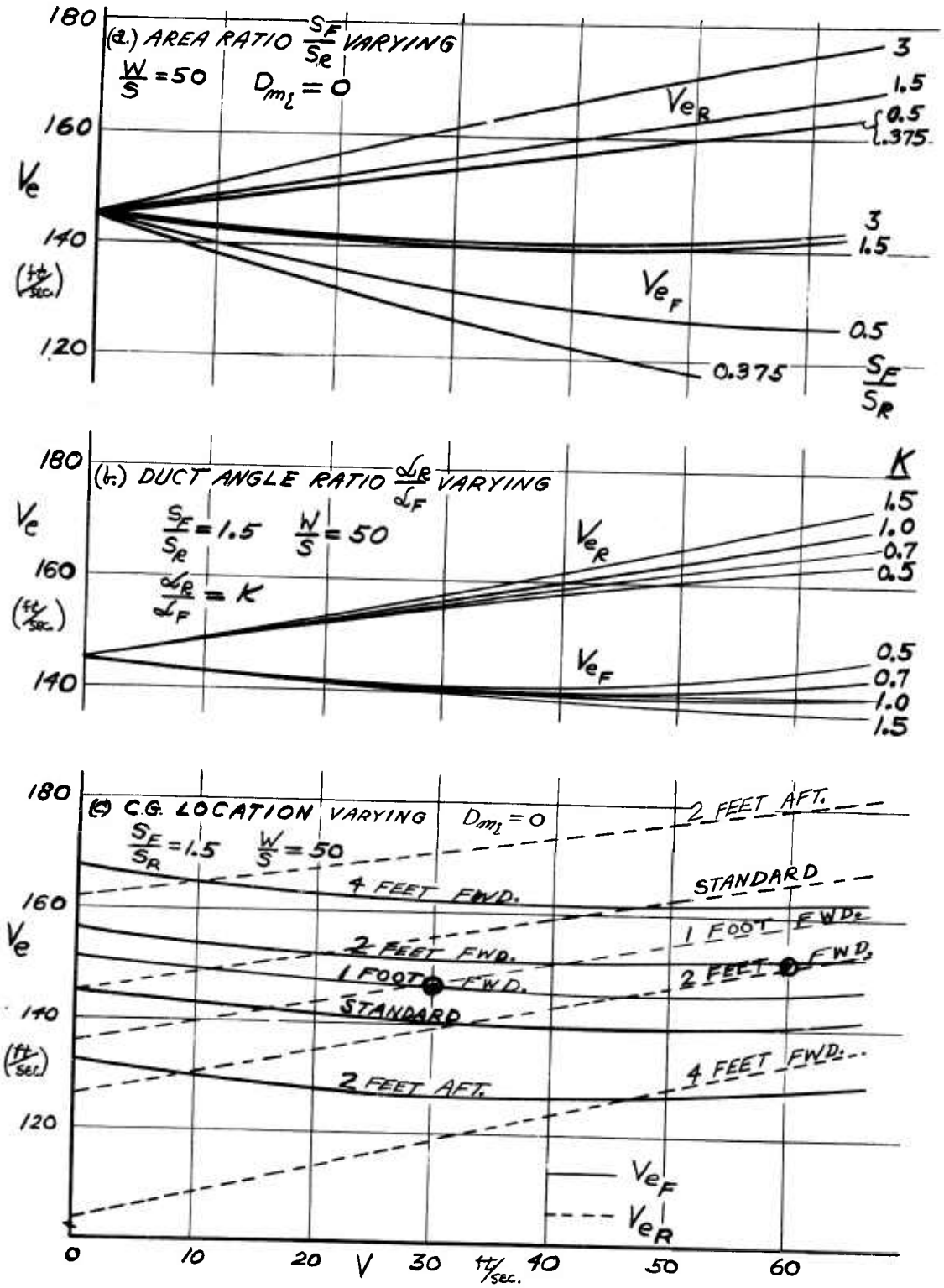

FIG. 7 DUCT EXIT VELOCITY vs. FORWARD SPEED

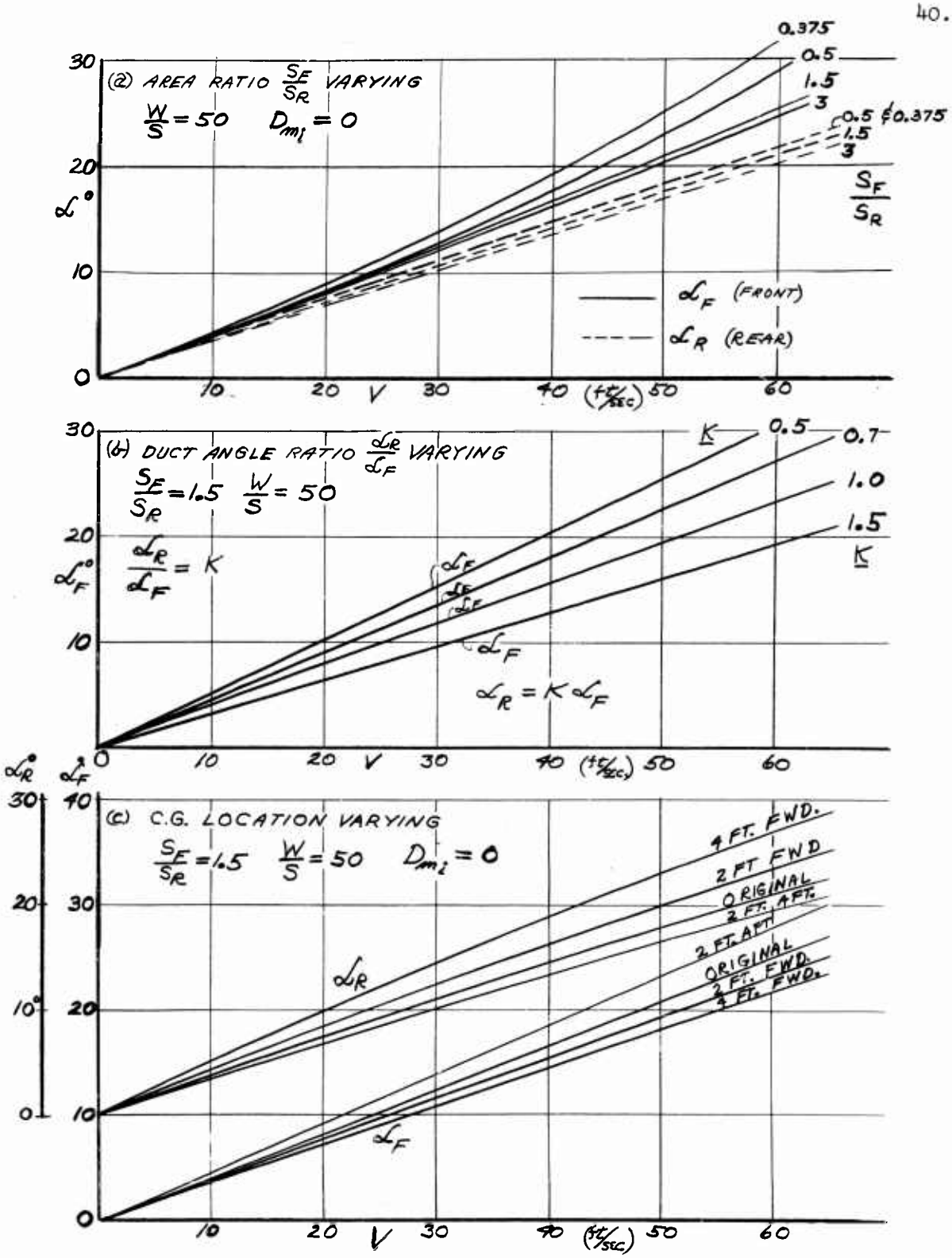

FIG. 8 DUCT ANGLE VS. FORWARD SPEED

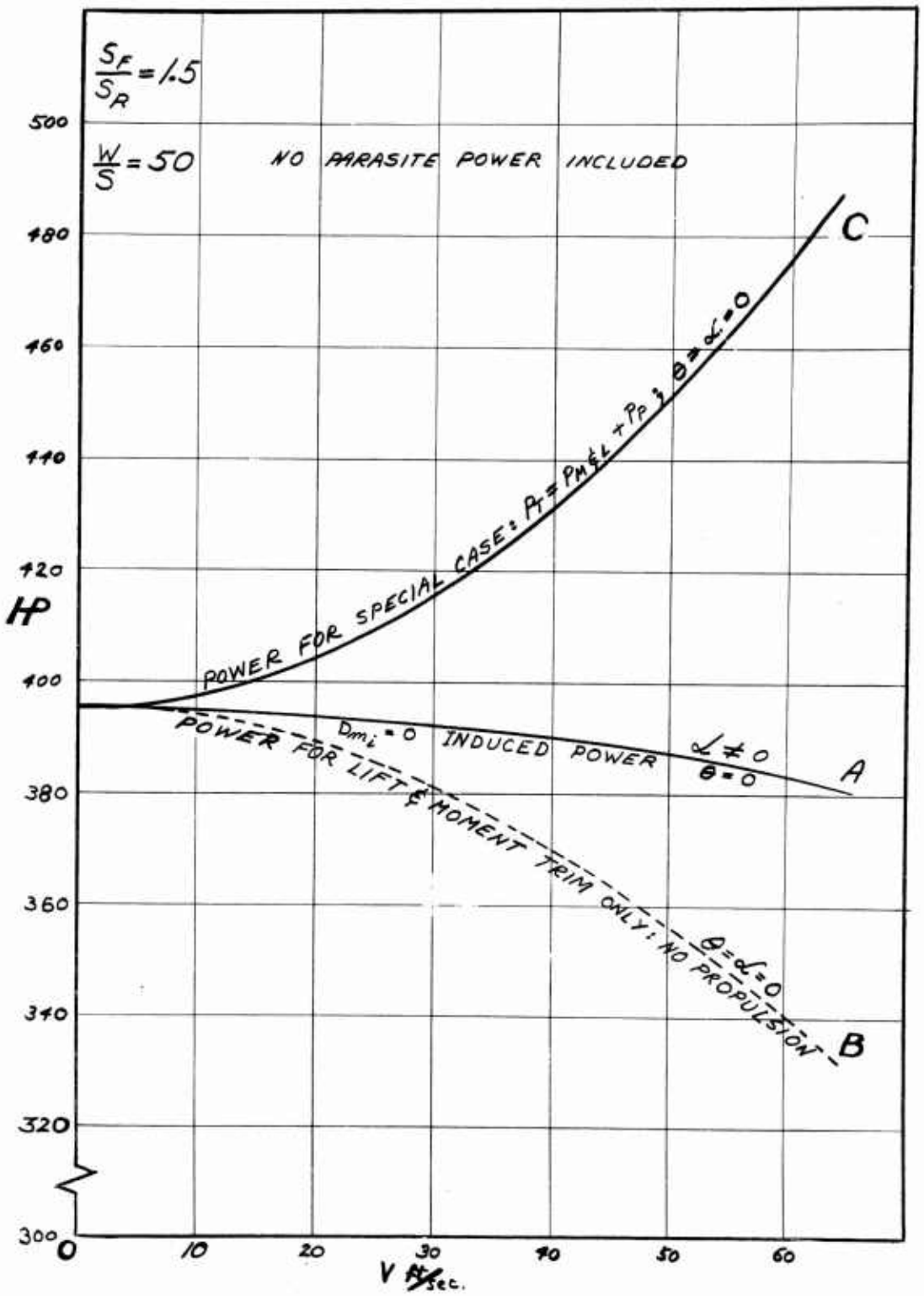

FIG. 9 SPECIAL CASE ($\alpha = \theta = 0$)

APPENDIX A

ITERATION PROCEDURE

CASE I

Iteration procedure used for obtaining solutions to the equilibrium trim equations for the case where the ducts are in individual momentum drag equilibrium, $D_{m_i} = 0$:

Steps

1. Select an α_1
2. Since $D_{m_i} = 0$, solve directly for $\frac{V}{V_{e_1}}$ by Equation (37)

$$\sin \alpha_1 = \frac{V}{V_{e_1}}$$

3. Assume an α_2
4. Similar to step 2, solve for $\frac{V}{V_{e_2}}$ by Equation (38).

$$\sin \alpha_2 = \frac{V}{V_{e_2}}$$

5. Knowing $\frac{V}{V_{e_1}}$ and $\frac{V}{V_{e_2}}$ from steps 2 and 4 find $\frac{V_{e_1}}{V_{e_2}}$ by

$$\frac{V}{V_{e_2}} \div \frac{V}{V_{e_1}} = \frac{V_{e_1}}{V_{e_2}}$$

6. Evaluate C_{L_1}, C_{L_2}, C_{M_1} and C_{M_2} (Equations (13) and (17)) using α_1, α_2, $\frac{V}{V_{e_1}}$ and $\frac{V}{V_{e_2}}$ obtained in steps 1 through 4.
7. Given c_1, c_2, S_1, S_2, l_1 and l_2, the moment equation (Eq. (32)) may be solved for $\frac{V_{e_1}}{V_{e_2}}$ by using the values obtained in step 6 for C_{L_1}, C_{L_2}, C_{M_1} and C_{M_2}.

8. Compare the value of $\frac{V_{e_1}}{V_{e_2}}$ obtained in step 7 to the value of $\frac{V_{e_1}}{V_{e_2}}$ obtained in step 5.

9. Repeat steps 3 to 8 inclusive (in step 3 assume another value for α_2) until the value of $\frac{V_{e_1}}{V_{e_2}}$ obtained in step 7 is equal to the value of $\frac{V_{e_1}}{V_{e_2}}$ obtained in step 5.

10. Express V_{e_2} in terms of V_{e_1} using the final value of $\frac{V_{e_1}}{V_{e_2}}$ $\left(\frac{V_{e_1}}{V_{e_2}} = C\right)$ as obtained in step 9. $V_{e_2} = \frac{V_{e_1}}{C}$

11. Substituting the expression of step 10 for $V_{e_2}^2$ in the lift equation (Equation (20)), solve the lift equation for V_{e_1} where W equals 3000 pounds, α_1 from step 1 and α_2 from the final value assumed in step 3.

$$W = \rho S_1 V_{e_1}^2 \cos \alpha_1 + 2 \rho S_2 \frac{V_{e_1}^2}{C^2} \cos \alpha_2$$

12. Using the value of V_{e_1} obtained in step 11 with the value of $\frac{V}{V_{e_1}}$ in step 2, solve for the forward speed by

$$\frac{V}{V_{e_1}} \cdot V_{e_1} = V$$

13. Knowing the final value of $\frac{V_{e_1}}{V_{e_2}}$ from step 9 find V_{e_2} using the value of V_{e_1} from step 11 as

$$V_{e_1} \div \frac{V_{e_1}}{V_{e_2}} = V_{e_2}$$

The final values of α_1, α_2 V_{e_1}, V_{e_2} and V are the solutions to the equations.

CASE II

Iteration procedure used for obtaining solutions to the equilibrium trim equations where the ducts are geared together so that $\alpha_2 = K\alpha_1$. In this case the duct angles α_1 and α_2 are programmed in a prescribed fashion where $\frac{\alpha_2}{\alpha_1}$ = K and K equals 0.5, 0.7, 1.0 and 1.5.

Steps

1. Since this case assumes a certain duct angle ratio K, select an α_1
2. Obtain α_2 from $\alpha_2 = K\alpha_1$.
3. In the drag equation (Equation (27)), expressing $\frac{V}{V_{e_1}}$ as $\frac{V}{V_{e_2}}$ divided by $\frac{V_{e_1}}{V_{e_2}}$ and non-dimensionalizing by $\rho S_2 V_{e_2}^2$, Equation (27) takes the form

$$0 = \frac{S_1}{S_2}\frac{V_{e_1}^2}{V_{e_2}^2}\left[\sin\alpha_1 - \frac{V/V_{e_2}}{V_{e_1}/V_{e_2}}\right] + 2\left[\sin\alpha_2 - \frac{V}{V_{e_2}}\right]$$

4. Solving the above equation for $\frac{V}{V_{e_2}}$

$$\frac{V}{V_{e_2}} = \frac{\frac{S_1}{S_2}\left(\frac{V_{e_1}}{V_{e_2}}\right)^2 \sin\alpha_1 + 2\sin\alpha_2}{\frac{S_1}{S_2}\frac{V_{e_1}}{V_{e_2}} + 2}$$

5. Assume a value for $\frac{V_{e_1}}{V_{e_2}}$
6. Solve the drag equation of step 4 for $\frac{V}{V_{e_2}}$ using the assumed value of $\frac{V_{e_1}}{V_{e_2}}$ of step 5.

7. Using $\frac{V}{V_{e_2}}$ of step 6 and $\frac{V_{e_1}}{V_{e_2}}$ of step 5, calculate the value of $\frac{V}{V_{e_1}}$ by

$$\frac{V}{V_{e_2}} \div \frac{V_{e_1}}{V_{e_2}} = \frac{V}{V_{e_1}}$$

8. Knowing $\frac{V}{V_{e_1}}$, $\frac{V}{V_{e_2}}$, α_1 and α_2 calculate values of C_{L_1}, C_{L_2}, C_{M_1} and C_{M_2} (Equations (13) and (17)).

9. Using the values of step 8, solve the moment equation (Equation (32)) for $\frac{V_{e_1}}{V_{e_2}}$.

10. Compare $\frac{V_{e_1}}{V_{e_2}}$ of step 9 to value of $\frac{V_{e_1}}{V_{e_2}}$ assumed in step 5.

11. Repeat steps 5 through 10 inclusive until the value of $\frac{V_{e_1}}{V_{e_2}}$ of step 10 is equal to the value of $\frac{V_{e_1}}{V_{e_2}}$ in step 5.

12. In obtaining the final value of $\frac{V_{e_1}}{V_{e_2}}$ in step 11, the final values of $\frac{V}{V_{e_1}}$ and $\frac{V}{V_{e_2}}$ have been obtained in steps 6 and 7.

13. The values of α_1 and α_2 are obtained from steps 1 and 2.

14. Using the final value of $\frac{V_{e_1}}{V_{e_2}}$, $\frac{V}{V_{e_1}}$, $\frac{V}{V_{e_2}}$, α_1 and α_2 (steps 11, 12 and 13), the remaining quantities V, V_{e_1} and V_{e_2} may be obtained by repeating the same method outlined in steps 10 through 13 of CASE I.

UNCLASSIFIED